

## Article

# A Comparative Study of the Rheological Properties of a Fly Ash-Based Geopolymer Reinforced with PP Fiber for 3D Printing: An Experimental and Numerical Approach

Bakytzhan Sariyev <sup>1,\*</sup> , Alisher Konysbekov <sup>2</sup>, Assel Jexembayeva <sup>3,\*</sup> and Marat Konkanov <sup>3</sup>

<sup>1</sup> Department of Mechanical and Aerospace Engineering, School of Engineering and Digital Sciences, Nazarbayev University, Nur-Sultan 010000, Kazakhstan

<sup>2</sup> Department of Civil Engineering, School of Engineering and Digital Sciences, Nazarbayev University, Nur-Sultan 010000, Kazakhstan

<sup>3</sup> Faculty of Architecture and Civil Engineering, Gumilyov Eurasian National University, Kazhymukan Str. 13 r205, Astana 010008, Kazakhstan; marcon@metrology.kz

\* Correspondence: bakytzhan.sariyev@nu.edu.kz (B.S.); dzheksembayeva\_ae@mail.ru (A.J.)

**Abstract:** The present study investigates the flow characteristics of fly ash-based (FA) geopolymers reinforced with polypropylene (PP) fibers during the extrusion process in three-dimensional printing. By applying the Herschel–Bulkley rheological model, this research provides a sound theoretical basis to understand the flow behavior of these materials under various conditions. The Herschel–Bulkley model describes the relationship between shear stress and the shear rate in non-Newtonian fluids, capturing yield stress and flow consistency. A combination of experimental and numerical techniques based on the Finite-Element Method (FEM) in COMSOL has been used in this study. The results of both experimental and simulation approaches are compared to examine the material behavior during extrusion. The experimental results indicate that PP fiber content significantly affects the rheological properties. Mixtures with high fiber content encountered issues such as high static yield. However, mixtures with moderate fiber content showed smoother extrusion processes, suggesting an optimal fiber addition range that balances mechanical properties and extrudability. The numerical simulations generally agreed with the experimental data up to a certain fiber content level, beyond which more complex interactions necessitate further model refinements. The investigation identified a 0.25% to 0.5% fiber content range that enhances performance without complicating the extrusion process, facilitating the production of properly printed structures.

**Keywords:** geopolymer; rheological properties; extrusion process; Herschel–Bulkley model; finite-element method (FEM)



**Citation:** Sariyev, B.; Konysbekov, A.; Jexembayeva, A.; Konkanov, M. A Comparative Study of the Rheological Properties of a Fly Ash-Based Geopolymer Reinforced with PP Fiber for 3D Printing: An Experimental and Numerical Approach. *Buildings* **2024**, *14*, 2068. <https://doi.org/10.3390/buildings14072068>

Academic Editor: Grzegorz Ludwik Golewski

Received: 21 May 2024

Revised: 17 June 2024

Accepted: 26 June 2024

Published: 6 July 2024



**Copyright:** © 2024 by the authors. Licensee MDPI, Basel, Switzerland. This article is an open access article distributed under the terms and conditions of the Creative Commons Attribution (CC BY) license (<https://creativecommons.org/licenses/by/4.0/>).

## 1. Introduction

The arrival of additive manufacturing technology has revolutionized the manufacturing world, enabling unprecedented complexity and productivity. This technology's effectiveness often depends on the rheological properties of the materials used, which determine their behavior during the extrusion process. Rheological properties refer to the flow behavior of materials under different stress conditions and are critical in additive manufacturing for ensuring smooth and consistent material extrusion [1].

Among the many materials, geopolymers are modern binders known for their mechanical properties, environmental benefits, and customization potential. Geopolymer concrete (GPC), derived from industrial wastes such as fly ash, may replace Portland cement in some applications, offering green and potentially superior alternatives, including 3D printing. However, these materials must be fully understood regarding their rheological behavior to print 3D parts effectively. The main challenge hindering the introduction of 3D printing of concrete is improving material characteristics [2–4].

Additives play a crucial role in enhancing concrete's structural properties and compressive strength. Traditional additives such as silica fume and slag have been widely used to improve concrete's durability, workability, and mechanical properties. Silica fume, for example, significantly increases compressive strength and reduces permeability by filling the micro-pores within the concrete matrix. The optimum percentage of silica-based additives generally ranges from 10–15% of the binder weight, balancing strength enhancement and workability [5,6]. Novel additives, including polypropylene fibers, carbon nanotubes, and nano-silica, offer further improvements by enhancing tensile strength, reducing shrinkage, and increasing resistance to cracking [7,8]. Polypropylene fibers, in particular, have been shown to improve the ductility and toughness of geopolymer composites, making them suitable for 3D printing applications [9–12]. The inclusion of polypropylene fibers was investigated in the literature, revealing that their influence is rather complex. In the main, PP fibers slightly enhanced interlayer bond strength and drastically increased composite ductility and tensile strength. These enhancements could be explained by the fiber's characteristic ability to absorb energy once it is deformed [13]. It is reported by [9] that there is a 0.8% PP fiber increase in flexure and tensile strength by 8.2% and 71.7%, respectively. According to Bellum [11], the composites reinforced by fiber exhibited an increasing flexural toughness index with rising PP content. The research conducted by Nematollahi et al. [10] also investigated the relation between the inclusion of PP fibers in concrete and the improvement observed for shape retention, compressive strength, shrinkage, and deformation of concrete.

Moreover, FEM is extensively used in simulating the behavior of these advanced materials under different loading conditions, helping to optimize the mix design and predict performance [14–16]. By incorporating the Herschel–Bulkley rheological model, FEM simulations can accurately represent the non-Newtonian flow behavior of fiber-reinforced geopolymers, which is essential for ensuring smooth extrusion and high-quality prints. Recent studies have demonstrated the effectiveness of FEM in predicting the flow behavior and structural performance of 3D-printed composites [17–19]. For instance, Murcia et al. (2021) investigated the rheological properties of 3D-printed geopolymer using FEM simulations to optimize the printing process [17]. Similarly, Venkatachalam et al. (2021) utilized FEM to study the numerical simulation of reinforced geopolymer concrete properties [18]. Additionally, a novel approach by Pishro et al. (2024) showcases the integration of FEM with machine learning to enhance the understanding of bond stress–slip behavior in ultra-high-performance concrete [19]. These studies collectively highlight the importance of integrating traditional and novel additives to enhance the performance of concrete and geopolymer composites in construction applications.

The significance of using fly ash lies in its environmental benefits, such as reducing industrial waste and carbon emissions. PP fibers are chosen for their ability to enhance mechanical properties, such as tensile strength and ductility, which are crucial for 3D-printed structures. Adding polypropylene fibers to fly ash-based geopolymer composites can influence the material's rheological properties through various chemical interactions. At the chemical level, the fibers may interact with the alkaline activators (sodium silicate and sodium hydroxide) used in the geopolymerization process. These interactions can alter the aluminosilicate network's formation and structure, affecting the mixture's viscosity and flow behavior. Specifically, fibers can disrupt the continuous gel phase, leading to increased yield stress and viscosity. Furthermore, the surface chemistry of the PP fibers, although primarily inert, can still influence the microstructure by providing nucleation sites for geopolymer gel formation. This interaction can enhance the mechanical interlocking between the fibers and the matrix, contributing to the observed changes in rheological properties. Additionally, the fibers can create a physical barrier that restricts the movement of the geopolymer matrix, further contributing to the increase in viscosity and shear-thinning behavior. These chemical and physical interactions collectively impact the extrudability and overall performance of the geopolymer composite. Generally, the fiber content significantly influences the rheological properties and the quality of the printed structures. Increased

fiber content generally increases yield stress and viscosity, affecting the material's flow behavior. This can result in challenges during extrusion, such as clogging and increased pressure requirements. However, an optimal fiber content range can enhance mechanical properties without compromising extrudability.

This research addresses the gaps by comprehensively analyzing the rheological properties and extrusion behavior of fly ash-based geopolymer composites reinforced with polypropylene fibers. The geopolymer mortars were prepared with different PP fibers in the range of 0.25%, 0.5%, 0.75%, and 1.0% by the volume fraction. In this paper, the Herschel–Bulkley rheological model is the theoretical foundation for the flow behavior of geopolymers under different conditions, which is the basis for our experimental and numerical analysis. The study identifies the optimal fiber content range that balances mechanical properties and extrudability, offering valuable insights for improving 3D printing processes in construction. By combining experimental and numerical approaches, this research enhances our understanding of material behavior, contributing to advancing additive manufacturing technologies.

## 2. Materials and Methods

### 2.1. Materials

Class F fly ash was used as an aluminosilicate precursor to prepare geopolymer mixtures complying with the ASTM C618-19 specifications [5]. The specific oxide contents in the fly ash, such as  $\text{SiO}_2$ ,  $\text{Al}_2\text{O}_3$ ,  $\text{Fe}_2\text{O}_3$ , and  $\text{CaO}$ , play a critical role in the geopolymerization process.  $\text{SiO}_2$  and  $\text{Al}_2\text{O}_3$  are essential for forming the aluminosilicate network, providing the primary binding structure of the geopolymer. High  $\text{SiO}_2$  content enhances the material's strength and durability, while  $\text{Al}_2\text{O}_3$  contributes to the geopolymer's setting and hardening characteristics.  $\text{Fe}_2\text{O}_3$  can influence the color and mechanical properties, while  $\text{CaO}$  content affects the geopolymer's early strength development and workability. The FA has the following oxide contents:  $\text{SiO}_2 + \text{Al}_2\text{O}_3 + \text{Fe}_2\text{O}_3$  with a total content of 50%,  $\text{CaO}$  content under 15%,  $\text{LOI}$  under 3%, and  $\text{SO}_3$  content under 2%. Its average particle size ( $d_{50}$ ) and Blaine-specific surface are 50  $\mu\text{m}$  and 400  $\text{m}^2/\text{kg}$ , respectively. The chemical parameters of the FA are described in Table 1.

**Table 1.** Chemical characteristics of the fly ash used.

Chemical Component	Fly Ash F (%)
Silicon dioxide ( $\text{SiO}_2$ )	51.5
Titanium dioxide ( $\text{TiO}_2$ )	0.9
Aluminum oxide ( $\text{Al}_2\text{O}_3$ )	17.2
Iron oxide ( $\text{Fe}_2\text{O}_3$ )	5.2
Magnesium oxide ( $\text{MgO}$ )	2.2
Calcium oxide ( $\text{CaO}$ )	14.3
Sodium oxide ( $\text{Na}_2\text{O}$ )	1.4
Potassium oxide ( $\text{K}_2\text{O}$ )	1.5
Sulfur trioxide ( $\text{SO}_3$ )	1.6
Other oxides	1.5
Loss on ignition ( $\text{LOI}$ )	2.7
Total	100

The polypropylene fibers used in this study have a diameter of 20–25 microns and a length of 8 mm, with a tensile strength of approximately 550 MPa. These fibers were chosen for their high tensile strength, flexibility, and chemical inertness, making them ideal for reinforcing geopolymers.

Sodium-based compounds such as sodium silicate ( $\text{Na}_2\text{SiO}_3$ ) and sodium hydroxide ( $\text{NaOH}$ ) were used to make the alkaline solutions obtained from Sigma Aldrich (St. Louis, MO, USA). The preparation of the alkaline solutions involves first dissolving  $\text{NaOH}$  pellets in water to create a 12 M  $\text{NaOH}$  solution. This process requires careful handling due to the

exothermic nature of NaOH dissolution. Once the NaOH solution was prepared, it was cooled to room temperature. Subsequently, the Na<sub>2</sub>SiO<sub>3</sub> solution, which contains 28% SiO<sub>2</sub>, 8% Na<sub>2</sub>O, and 65% water, was mixed with the NaOH solution in a 1:1 ratio. However, an alkaline solution-to-binder ratio (S/B ratio) was taken as 0.4 for all geopolymer mixes.

### 2.2. Mix Proportions

The geopolymer composite mixes were made concerning the literature [20]. The PP fibers were incorporated into the geopolymer mixtures by first dry mixing them with the fly ash to ensure even distribution. This step is crucial to prevent fiber clumping. The dry mixture was then combined with the alkaline solution and mixed thoroughly using a mechanical mixer. The mixing process was carried out at a slow speed initially to avoid entanglement of the fibers and then at a higher speed to ensure uniform dispersion of the fibers throughout the geopolymer matrix. Table 2 shows the ratio of the materials used to produce the fiber-reinforced geopolymer composites. The fibers were introduced to the geopolymer binder as a weight fraction ratio of 0.25%, 0.5%, 0.75%, and 1%. The geopolymer mixture ID notations represent PP for polypropylene fibers. The number of fibers was the most favored condition according to the previous literature [10,11] to study the effect of the similar ratios of PP on the rheological properties of the geopolymer mortar.

**Table 2.** Geopolymer mixture proportions in 1000 g.

Mix ID	Binder (g)	Fiber (Volume %)	Na <sub>2</sub> SiO <sub>3</sub> (mL)	NaOH (mL)
PP0	710	0	142	142
PP0.25	710	0.25	142	142
PP0.5	710	0.5	142	142
PP0.75	710	0.75	142	142
PP1	710	1	142	142

### 2.3. Extrudability

In concrete printing, extrudability is the property of the material being pumped out effortlessly through an extruder, ensuring the pipe flow is not disrupted or clogged. According to this phenomenon related to the material's new property, many authors have characterized it with the Herschel–Bulkley parameters and other flow properties [12,21]. These studies show that the materials with very high yield stress are hard to extrude and may cause discontinuities during the extrusion process, which is the background of the type of pump used.

In the literature, it is seen that particle size, gradation, surface area, and paste/aggregate volume are the factors that control the yield stress and viscosity of the material, which can be connected to the flow properties inside any pipe or complex-shaped channel [22,23]. Besides, some standard tests like the flow table test and drop test [24] were previously employed by researchers to measure the flow behavior; in this study, the data obtained from the rheometer were used to investigate the extrudability of our custom-made geopolymer mortar developed for 3D printing application. Five different mixes, as presented in Table 2, were tested using the Anton Paar MCR 102 rotational rheometer by a parallel plate according to [25], and their respective Herschel–Bulkley parameters were noted. The rheological tests were conducted to evaluate the flow properties of the geopolymer mixtures. The setup involved using a parallel plate configuration with a plate diameter of 25 mm and a gap setting of 1 mm, performed at a controlled temperature of 25 °C to ensure consistency in the results. The rheometer was calibrated before each set of measurements using a standard oil with known viscosity. The flow curves were obtained by applying a range of shear rates from 0.1 to 100 s<sup>-1</sup>, allowing the determination of key parameters such as yield stress, viscosity, and the flow behavior index. The data collected provided insights into the shear-thinning behavior of the geopolymer mixtures, which is crucial for their application in 3D printing processes. Afterward, these mixtures were extruded out by a ram extruder

to align the rheology data for a good extrusion criterion. An example of the rheometer used in this paper is depicted in Figure 1.



**Figure 1.** Anton Paar MCR 102 rheometer used for fresh material property testing.

A ram extruder system with a rigid barrel with a smooth surface was made to investigate the rheology properties of fresh cementitious composites. The ram extruder setup used for testing the extrusion properties of the geopolymer mixtures consisted of a cylindrical barrel with an internal diameter of 40 mm and a length of 200 mm. The barrel was filled with fresh geopolymer composite, and a piston was used to apply pressure at a controlled rate. The nozzle attached to the barrel had a length of 64 mm and a diameter of 8 mm [2]. The extrusion tests were performed at various ram velocities, ranging from 5 mm/s to 30 mm/s, to assess the influence of extrusion speed on the flow behavior and pressure requirements. The data were recorded using pressure sensors positioned at the top of the barrel, providing real-time measurements of the extrusion pressure as a function of ram displacement and velocity [1]. This setup allowed for a detailed analysis of the extrudability of the geopolymer composites under different conditions [26]. The setup and schematic of the ram extruder are depicted in Figures 2, 3 and 4, respectively.

A standard experiment was conducted as follows: The barrel of the extruder with a length of 200 mm was filled with a specific amount of fresh composites until the brim of the barrel, and the piston was placed so that the crosshead of the test machine was in direct contact with the upper surface of the GPC in the barrel. This piston set was used as the reference point for the displacement [27]. The compression started at a constant speed. The program was designed to set a certain displacement (20 mm under the piston velocity of 0.1 mm/s in this study), followed by the extrusion procedure with different velocities [25]. Upon completing a test, the crosshead was shifted from the top of the GPC, and the extruder assembly was removed from the frame.

In this research, a constant initial height of the geopolymer in the barrel was used in all the experiments. Each composite mixture's nozzle length and diameter were 64 mm and 8 mm, respectively [10]. The extrusion pressure was measured as a function of time and ram displacement under a series of ram velocities of 5 mm/s, 10 mm/s, 15 mm/s, 20 mm/s, 25 mm/s, and 30 mm/s. A systematic flow chart of the aforementioned methods for laboratory testing 3D-printable GPC is shown in Figure 5.

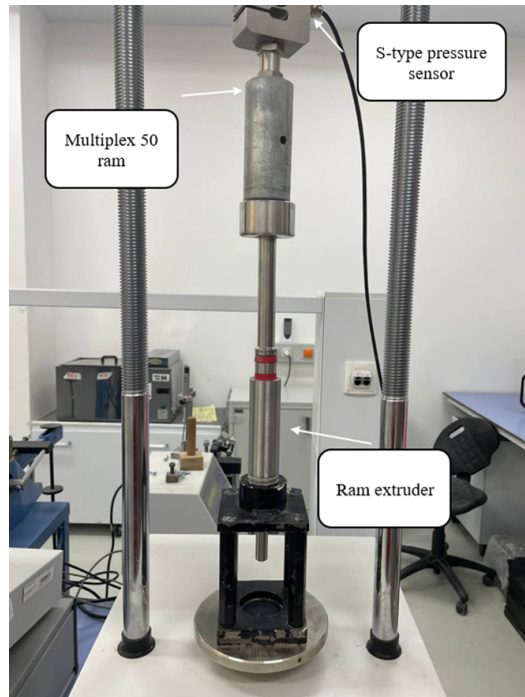


Figure 2. The setup of the ram extruder.

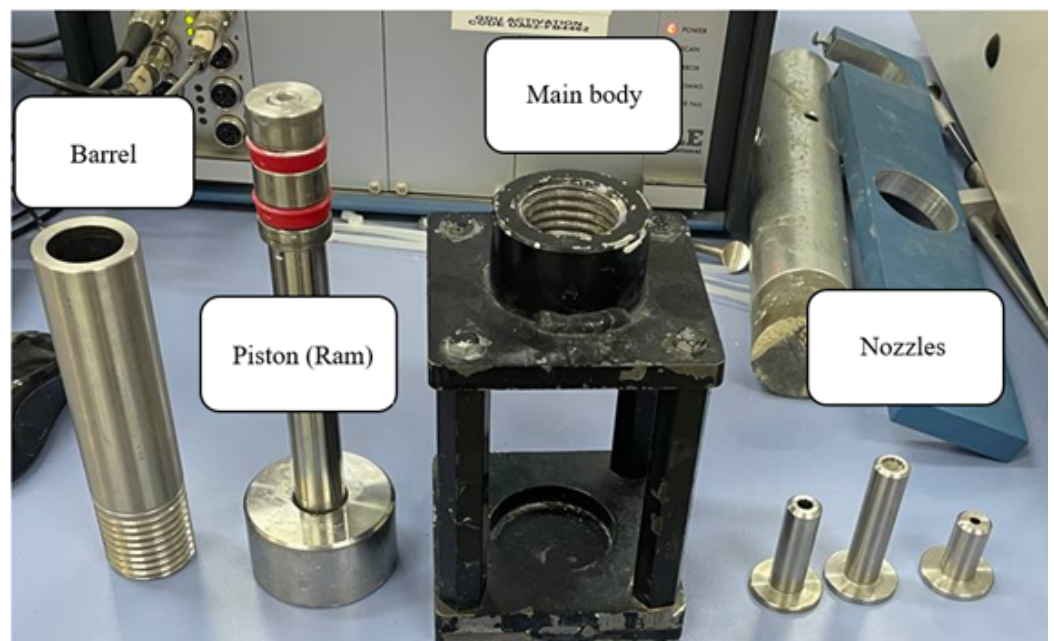
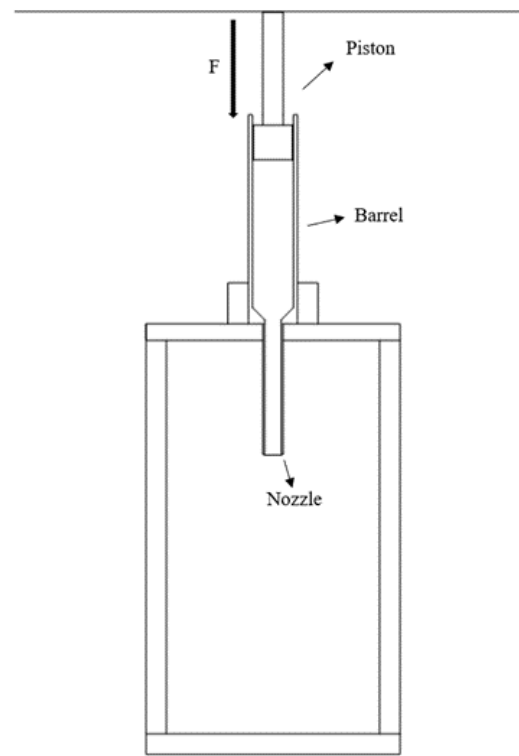
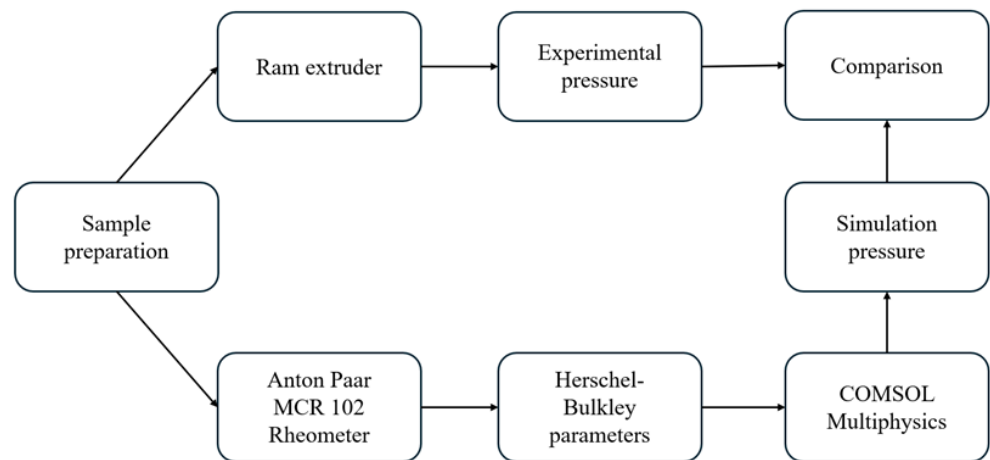


Figure 3. Components of the ram extruder.



**Figure 4.** Schematic of ram extruder.



**Figure 5.** The flow chart of experimental methods.

#### 2.4. Numerical Model

The simulation of the ram-extrusion process leverages the Lagrange method for the moving mesh, which is essential in finite-element analyses that deal with significant deformations or displacements. This method ensures that the simulation remains accurate as the material undergoes extensive shape changes during extrusion. While the Lagrange method is used to accurately track the deformation and flow of the material through the extrusion die, the simulation also incorporates a detailed model to describe the rheological behavior of the fluid, particularly focusing on its non-Newtonian characteristics [28].

The GPC numerical analysis was conducted using the COMSOL Multiphysics software. The parameters set for the simulation included a density of  $2300 \text{ kg/m}^3$ , a dynamic viscosity of  $0.01 \text{ Pa}\cdot\text{s}$ , and a yield stress of  $30 \text{ Pa}$  for the base geopolymer mixture. The Herschel–Bulkley parameters were adjusted according to the experimental results for each fiber content, with the consistency index ( $K$ ) and flow index ( $n$ ) values derived from the

rheological tests. The simulation also incorporated a moving mesh algorithm to account for the deformation and flow of the material through the extrusion die.

The Lagrange method can be described by the material derivative of the position vector  $\mathbf{X}$  of a particle (which corresponds to a mesh point) [29]:

$$\frac{D\mathbf{X}}{Dt} = \mathbf{v}(\mathbf{X}, t) \quad (1)$$

where  $\mathbf{v}(\mathbf{X}, t)$  is the velocity field of the material or fluid at position  $\mathbf{X}$  and time  $t$  [30].

For fluid dynamics, the velocity field  $\mathbf{v}$  must satisfy the Navier–Stokes equations, which for an incompressible fluid are given by:

$$\rho \left( \frac{\partial \mathbf{v}}{\partial t} + \mathbf{v} \cdot \nabla \mathbf{v} \right) = -\nabla p + \mu \nabla^2 \mathbf{v} + \mathbf{f} \quad (2)$$

$$\nabla \cdot \mathbf{v} = 0 \quad (3)$$

where  $\rho$  is the fluid density,  $p$  is the pressure,  $\mu$  is the dynamic viscosity, and  $\mathbf{f}$  is the body force (e.g., gravity) [31].

In the Lagrange method for the moving mesh, the mesh update equation is defined as:

$$\mathbf{X}_{\text{new}} = \mathbf{X}_{\text{old}} + \mathbf{v} \Delta t \quad (4)$$

where  $\mathbf{v}$  is the velocity field and  $\Delta t$  is the time step dictating the repositioning of mesh nodes according to fluid or material flow [32].

To optimize the mesh quality and minimize distortion, a variational approach is employed to minimize the gradient of mesh displacement:

$$\min_{\mathbf{X}} \int_{\Omega} \|\nabla \mathbf{X}\|^2 d\Omega \quad (5)$$

The Herschel–Bulkley model is employed to characterize the flow behavior of geopolymer mixtures due to its ability to accurately describe non-Newtonian fluids that exhibit both yield stress and shear-thinning behavior [12]. This model is particularly suitable for materials like geopolymers, which do not begin to flow until a certain yield stress is surpassed and then show a decrease in viscosity with increasing shear rates. The Herschel–Bulkley equation is given by:

$$\tau = \tau_y + K\dot{\gamma}^n \quad (6)$$

where  $\tau$  is the shear stress,  $\tau_y$  is the yield stress,  $K$  is the consistency index,  $\dot{\gamma}$  is the shear rate, and  $n$  is the flow index. This equation provides a comprehensive framework to capture these characteristics. This model helps understand how the material will behave under different processing conditions, essential for optimizing the extrusion process in 3D printing. To further enhance the representation of the material's complex flow behavior, the Herschel–Bulkley model can be extended with the Papanastasiou regularization [27,28]. This extended model, known as the Herschel–Bulkley–Papanastasiou model, allows for a more detailed depiction of the transition from solid-like to fluid-like behavior.

The Herschel–Bulkley–Papanastasiou model is particularly utilized to represent the complex flow behavior of the material. This model is expressed by Equation (7):

$$\tau = \tau_y (1 - e^{-m\dot{\gamma}}) + K\dot{\gamma}^n \quad (7)$$

Here,  $\tau$  is the shear stress acted upon by the fluid and  $\tau_y$  is the yield stress, the stress value below which flow cannot occur. The expression  $e^{-m\dot{\gamma}}$  shows the decay of the yield stress with an increment of the rates of shear  $\dot{\gamma}$ , where  $m$  is a modulating parameter that dictates how quickly the material will transition from a solid-like to a fluid-like behavior with increasing shear rate. The latter half of the equation,  $K\dot{\gamma}^n$ , describes the behavior of a fluid once it has started moving. These parameters are the consistency index  $K$  and

the flow behavior index  $n$ , which indicate the proportion of viscous behavior at several shear rates. The flow behavior index  $n$  is used to highlight whether the flow is shear-thinning ( $n < 1$ ), shear-thickening ( $n > 1$ ), or Newtonian ( $n = 1$ ). The design of this part of the model is important in determining the behavior of the material under various conditions during processing; as such, the processing pressure will be different from that applied for other materials, and the final product attributes will also vary. By incorporating the Herschel–Bulkley–Papanastasiou model, the simulation can properly depict the non-Newtonian rheology of the material, providing a framework for mesh movement synchronization with the material’s behavior throughout the simulation. This precise requirement determines the mechanical properties and strength of the extruded object [33].

Figure 6 provides visual representations of various flow behaviors to illustrate these concepts further. It includes the Newtonian model, where shear stress increases linearly with shear rate; the Power Law model, which depicts non-linear increases; the Bingham Plastic model, indicating a yield stress followed by linear behavior; and the Herschel–Bulkley model, which combines yield stress with non-linear shear-thinning or shear-thickening behavior. This figure helps understand the differences between these models, emphasizing how the Herschel–Bulkley model can accurately represent complex rheological behavior by accounting for yield stress and varying shear rates [28,34].

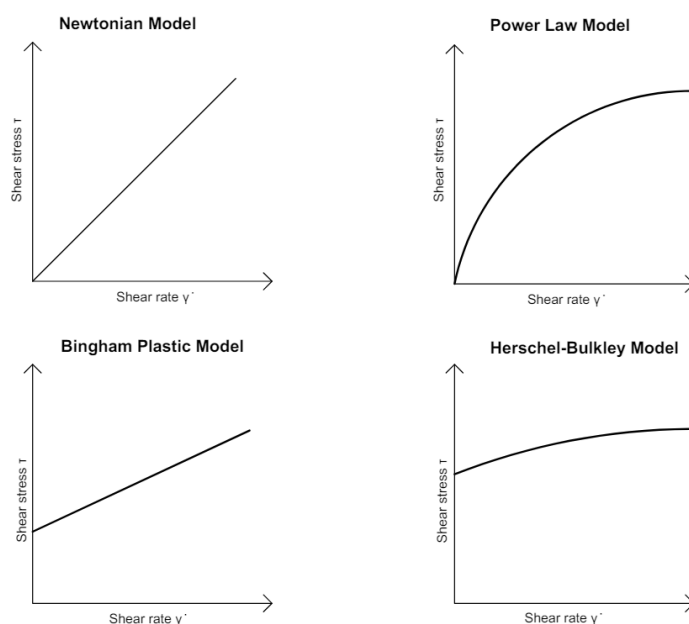


**Figure 6.** Rheological models [28].

### 2.5. Calibration and Validation of Numerical Model

The numerical model in COMSOL was calibrated and validated by comparing the simulation results with the experimental data. The calibration process involved adjusting the model parameters to match the experimental observations closely. The validation confirmed the model’s accuracy by reproducing the experimental results under various conditions. This approach ensured that the simulations reliably represented the rheological behavior of the geopolymer composites during extrusion.

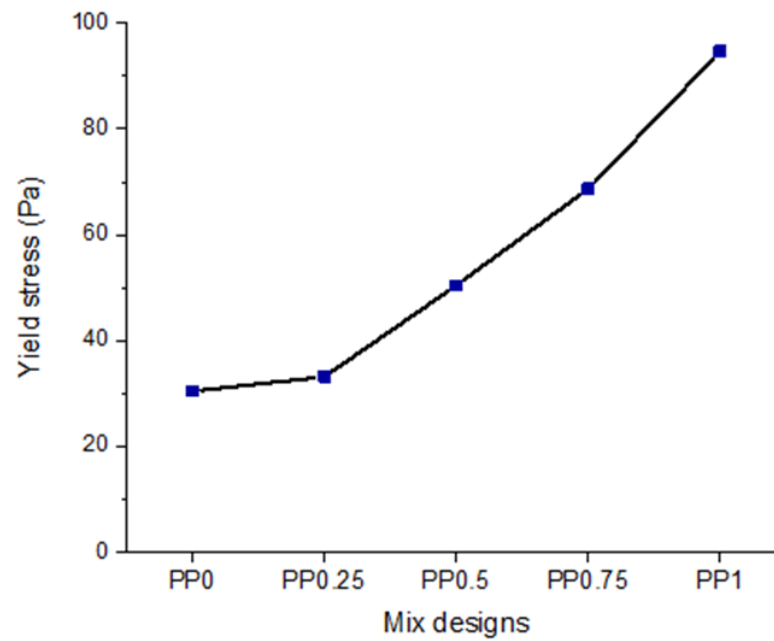
## 3. Results and Discussion

### 3.1. Experimental Results

The incremental adjustment of the PP fiber-to-binder ratio from 0 to 1 markedly impacted the extrudability of the mixes. Specifically, the mixes with 0.75% fiber (PP0.75) and those containing 1% (PP1) fiber encountered substantial challenges due to the need for high pressures at the outlet, measured at approximately 4–5 MPa, attributed to their high static

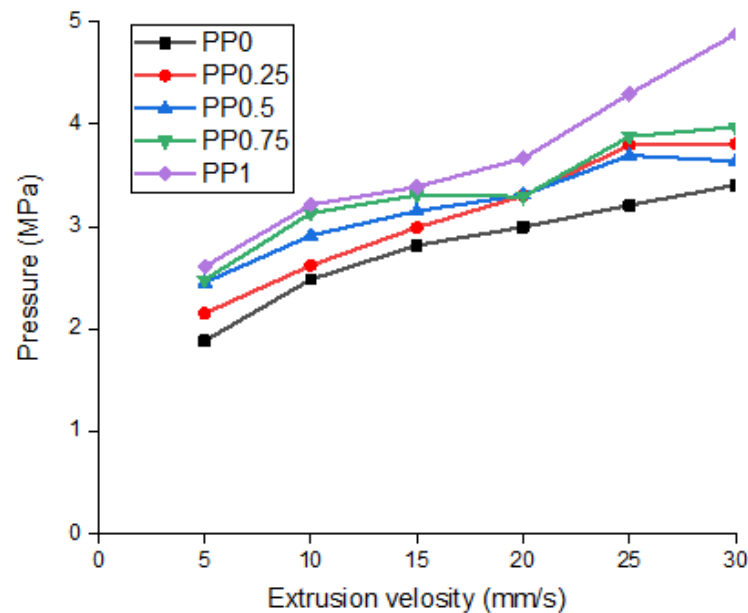
yield stress. Static yield stress refers to the minimum stress required to initiate flow in a material that behaves as a solid under lower stresses. Efforts to remedy these difficulties by adding extra water, approximately 5% by weight of the binder, did not yield successful results. The water was incrementally added and thoroughly mixed into the geopolymer paste to ensure homogeneity, but this approach led to further segregation and did not improve extrudability [35]. Furthermore, high shear forces within the piston caused material segregation in the mixes containing 0.75% (PP0.75) and 1% (PP1) fiber, suggesting that such high fiber-to-binder ratios are too excessive for effective geopolymer extrusion at the given binder volume. On the other hand, mixes with 0.25% (PP0.25) and 0.5% (PP0.5) fiber demonstrated smooth and continuous extrusion. Despite challenges with the PP1 fiber mix, the PP0.75 fiber mix was still extrudable under the current conditions. The difficulties in extruding the PP1 fiber mix were primarily due to the need for higher pressures to initiate flow, as indicated by the high static yield stresses. High static yield stresses frequently present challenges in extrusion processes due to thixotropic materials, which complicate extrusion under static conditions, but become less viscous under shear. Thixotropic materials are materials that decrease in viscosity over time when subjected to a constant shear rate. This challenge was intensified by the increased fiber-to-binder ratio, leading to greater material interference and ultimately clogging the nozzle. Material segregation in the PP0.75 and PP1 fiber mixes was identified through visual observations and extrusion pressure data. During the extrusion process, visible fiber clumps and non-uniform flow indicated segregation. Additionally, fluctuations in extrusion pressure, recorded by pressure sensors, suggested inconsistent material flow and segregation. Post-extrusion examination of the printed structures also revealed uneven fiber distribution and surface irregularities, confirming the occurrence of segregation.

Figure 7 illustrates the static yield stresses of the geopolymer mixes with varying fiber contents. The yield stress increases with fiber content, indicating higher resistance to initial flow. The PP0 mix had a yield stress of approximately 30 Pa, while the PP1 mix exhibited a yield stress of around 95 Pa. These results highlight that higher fiber content increases yield stress, making extrusion more challenging. Mixes with the PP0.25 and PP0.5 fiber demonstrated smoother and continuous extrusion, whereas mixes with the PP0.75 and PP1 fiber encountered significant flow resistance and material segregation. The experimental findings suggest that a static yield stress range of 30–70 Pa is optimal for smooth extrusion of the geopolymer mortar, with the PP0.5 fiber mix identified as the most effective within this parameter range.



**Figure 7.** Static yield stresses of the geopolymer mixes.

The extrusion rheometric test was conducted on all mixes, as depicted in Figure 8, illustrating the extrusion pressure data. The linear nature of the plot suggests that the GPC was thoroughly mixed and that the die land flow was completely established at the die entrance.



**Figure 8.** Effect of PP contents on extrusion pressure.

This graph presents the relationship between extruder velocity and extrusion pressure for GPC with varying fiber content. As illustrated, the extrusion pressure increases with the extruder velocity for all GPC mixes. Additionally, including fibers elevates the extrusion pressure across most velocities, making the effect more significant as the fiber content increases. This suggests that fiber adds resistance to flow in the paste, necessitating higher pressures for extrusion, particularly at higher velocities and fiber concentrations.

### 3.2. Rheological Parameters

By fitting the Herschel–Bulkley regression model to the experimental data from the flow curve, critical parameters are extracted, enhancing the understanding of the flow properties of these fiber-reinforced mixes. The Herschel–Bulkley model was used to characterize the rheological behavior of the geopolymer mixtures. The model parameters, including yield stress  $\tau_y$ , consistency index  $K$ , and flow index  $n$ , were derived from the experimental data. The experimental results aligned with the theoretical expectations, with the model accurately capturing the shear-thinning behavior of the mixtures. For instance, the yield stress and consistency index increased with fiber content, which was consistent with the theoretical predictions. The flow index values indicated shear-thinning behavior ( $n < 1$ ), which aligned with the observed decrease in viscosity at higher shear rates. This shear-thinning behavior is beneficial for extrusion processes, as it allows the material to flow more easily under applied stress, reducing the risk of clogging and ensuring a smoother extrusion process.

Figure 9 illustrates how shear stress responds to changes in the shear rate for GPC with different fiber contents. All the curves exhibit a similar behavior: a sharp decrease in shear stress at low shear rates, followed by a leveling off as the shear rate increases. This pattern indicates that all mixtures display shear-thinning behavior, where they become less viscous under higher shear rates. Initially, the GPC with no fiber shows the lowest shear stress, but the initial shear stress increases slightly as fiber content increases. After the steep initial drop, the curves flatten and run closely at higher shear rates, suggesting that the fiber's impact on resistance to flow becomes less pronounced as the shear rate increases. This graph underscores the influence of fiber content on the flow properties of different mixtures, particularly under different mechanical stress conditions. After the regression analysis of the curves, the Herschel–Bulkley parameters are derived. Table 3 shows the parameters for each mixture.

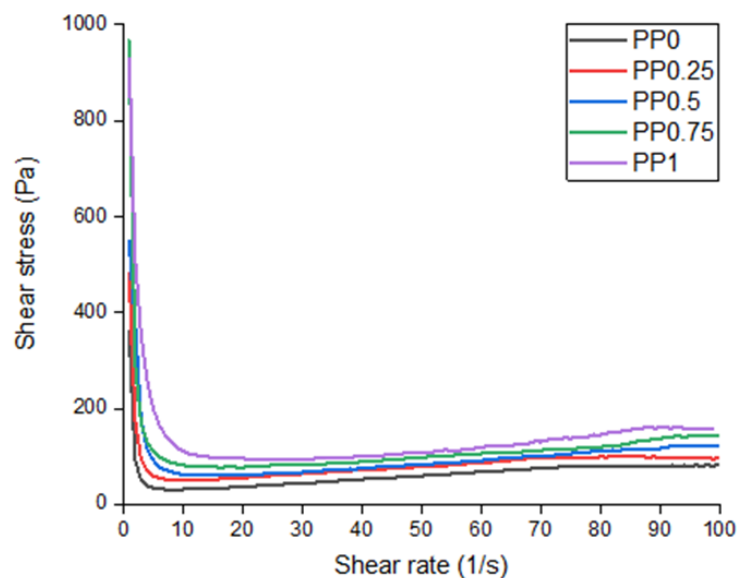


**Figure 9.** Plot of shear stress vs. shear rate of the geopolymer mixtures.

**Table 3.** Rheological parameters of mixture.

Mix ID	Yield Stress, $\tau_y$ (Pa)	Consistency Index, $K$ ( $\text{Pa}\cdot\text{s}^n$ )	Flow Index, $n$
PP0	30.416	5.59	0.719
PP0.25	33.172	6.68	0.708
PP0.5	50.464	8.44	0.698
PP0.75	68.694	12.52	0.657
PP1	94.655	10.13	0.684

For the Herschel–Bulkley rheological parameters—yield stress, consistency index, and flow index—for GPC with varying fiber contents, a clear trend is observable: as fiber content increases, yield stress also rises significantly, nearly tripling from 30.416 with no fiber to 94.655 with 1% fiber, indicating that fiber reinforcement enhances the paste's resistance to initial deformation under stress. The consistency index, which measures the viscosity, similarly increases from 5.59 to 10.13 as the fiber content is raised to 1%, reflecting a thicker or more viscous consistency. In contrast, the flow index decreases with higher fiber content, moving from 0.719 to 0.684. This suggests a transition from Newtonian, where the value is closer to 1, to more pronounced shear-thinning behavior.

### 3.3. Comparative Analysis

Figure 10 shows all mixtures' experimental and simulation data. For the GPC with no fiber, Figure 10a illustrates a close match between the experimental and simulated data across all velocities. This consistency suggests that the model used effectively captures the rheological behavior of the fiber-free mixture under various extrusion velocities. Both curves exhibit a generally linear relationship with a slight non-linearity as velocity increases, indicating a consistent increase in pressure with velocity. The correlation between the two curves reaffirms the reliability of simulations in predicting extrusion pressures in fiber-free conditions. Figure 10b for the GPC containing 0.25% fiber shows a strong correlation between the experimental and COMSOL data, with both curves rising steadily as the velocity increases. Introducing a small amount of fiber appears to slightly increase the pressure required at higher velocities than the fiber-free mixture, reflecting the beginning of increased resistance due to the fiber content. However, the low fiber concentration keeps this effect relatively mild, making the simulation model accurate. Regarding PP0.5, there is a noticeable increase in pressure as the fiber content increases. This graph shows slight deviations between the experimental and simulation results, especially at higher velocities. This deviation could suggest that the model's assumptions are less accurate at capturing the interactions between the fibers and the matrix at medium fiber concentrations, particularly under higher shear conditions in the extrusion process. The PP0.75 mixture illustrates an even greater increase in pressure as the velocity increases, with noticeable discrepancies between the experimental and simulation data starting around 20 mm/s. The pressure drop observed at 20 mm/s for the PP0.75 mixture can be explained by the onset of fiber alignment within the flow. At this velocity, the shear forces are sufficient to align the fibers in the flow direction, reducing the resistance to extrusion and causing a temporary pressure drop. However, as the velocity increases, the interaction between the aligned fibers and the matrix increases, leading to a subsequent rise in pressure. This phenomenon highlights the complex interplay between fiber orientation and flow behavior in fiber-reinforced composites. Notable discrepancies between experimental and simulation results were observed at higher fiber contents (PP0.75 and PP1). Possible reasons for these discrepancies include the limitations of the simulation model in capturing complex fiber–matrix interactions, fiber aggregation, and alignment issues that are more pronounced at higher fiber contents. Additionally, the simulation may not fully account for the thixotropic behavior of the mixtures, leading to deviations in predicted extrusion pressures. These factors suggest the need for further refinement of the numerical model to represent the behavior of high-fiber-content pastes better. This suggests that more fiber introduces complexities, such as possible fiber aggregation or alignment issues, which are not fully accounted for in the simulation model. The increased fiber content may be approaching a threshold where fiber–fiber interactions significantly influence the flow characteristics. To better capture the behavior of high-fiber-content pastes, the COMSOL model can be improved by incorporating more detailed fiber–matrix interaction mechanisms and accounting for fiber orientation and distribution. Including a sub-model to represent the mixtures' thixotropic behavior would enhance the simulations' accuracy. Additionally, refining the mesh and using adaptive meshing techniques can help accurately capture the localized effects of fiber aggregation and alignment. These improvements would enable the model to better predict

the extrusion behavior of high-fiber-content geopolymers. Finally, Figure 10e with 1% fiber shows the largest differences between the experimental and numerical results, particularly at higher velocities. This indicates significant challenges in modeling the behavior of high-fiber-content pastes. The steep rise in pressure with velocity in the experimental data suggests that the fibers could be causing substantial resistance, likely due to entanglements or blockages within the extrusion equipment. The simulation underpredicts this resistance, highlighting a potential area for model improvement. The findings underscore the critical balance required in fiber-reinforced geopolymers. While fibers can enhance certain properties like tensile strength and crack resistance, their impact on the extrusion process can be detrimental if not properly managed. It is clear from the data that an effective range of fiber content enhances performance without overly complicating the extrusion process—likely near 0.25% and 0.5%, based on the current data set.

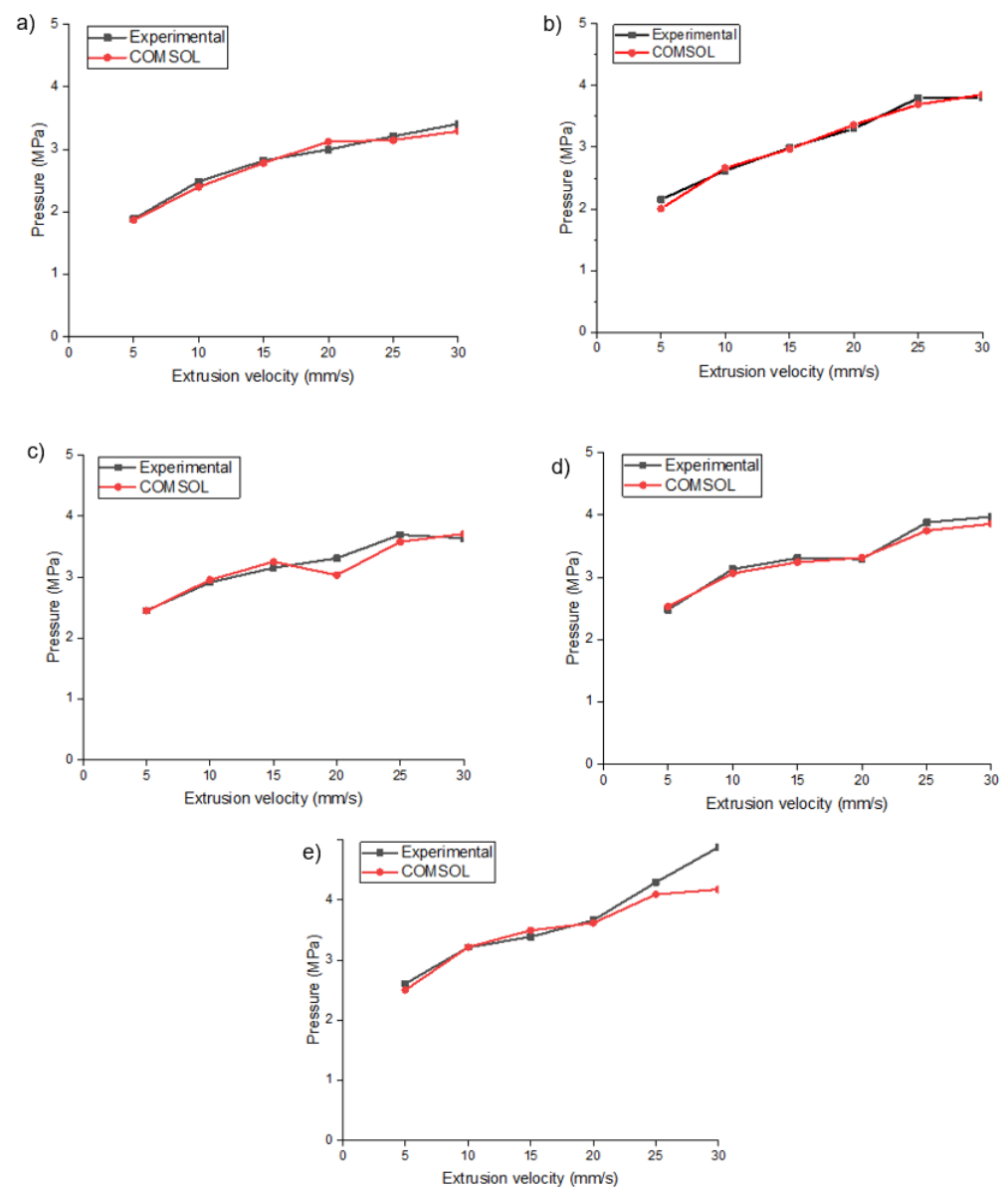


**Figure 10.** Comparative plot of experimental and numerical approach for (a) PP0, (b) PP0.25, (c) PP0.5, (d) PP0.75, and (e) PP1 mixtures.

This research considers the detailed investigation of the rheological properties of fly ash-based geopolymer composites reinforced with polypropylene fibers as the main topic

of analysis on which the behavior of these materials during the extrusion process for 3D printing applications is considered. Efficiently using the Herschel–Bulkley formulation, the study holds the key to capturing the behavior of these materials in non-Newtonian flow, which is very essential for optimizing their performance during additive manufacturing. The experimental result shows that the geopolymer composites' extrudability and rheology properties vary drastically with the PP fiber content. The mix without fibers, PP0, among all fiber contents and the ones with the highest fiber content, PP1, encountered significant problems during extrusion because of high static yield stress, resulting in increased pressures that almost always caused jamming and segregation of materials. On the other hand, mixes of fiber with a low–moderate fiber content, PP0.25 and PP0.5, show smoother extrusion processes within the phase, thus providing a range of fiber addition efficiency that is effective for improving mechanical properties with better extrudability. The rheological tests showed that the yield stress and consistency index of the formulae were mostly increased by adding fibers; thus, the behavior tends to become more viscous and shear-thinning. It was particularly noticeable for blends with increased fiber content, which decreased the flow index, indicating increased resistance to deformation under compression. This shows that the results of the Herschel–Bulkley model in the fiber-reinforced geopolymers' flow characterization agree with the theoretical predictions, thus pointing to the applicability of this model in the field. The FEM simulations run in COMSOL enabled a numerical approach to the flow pattern in the PP-reinforced geopolymer, which gave a good overview. The simulation results were in the same order as the experimental data results for low to moderate fiber contents. The existence of these differences stresses the complexities resulting from fiber interactions. It unifies the requirements for improvement in the simulation models to accurately portray the behavior of fiber-filled mixes. Fibers in the geopolymer structure play a major role in attaining the needed extrudability and mechanical properties crucial for using the material in 3D printing. The research identifies the fiber content range that meets the need for improving structural performance and soon-to-be-model components' quality by balancing the extrusion pressure and minimizing pressure spikes. Such a balance is inseparable from the evolution of geopolymers in construction, where the ability to manage material properties with precision is essentially the key to creating reliable and durable 3D-printed structures.

#### 4. Conclusions

In this study, the rheological properties and extrusion behavior of fly ash-based geopolymer composites reinforced with polypropylene fibers were comprehensively analyzed. The key findings are summarized as follows:

- The Herschel–Bulkley rheological model accurately described the non-Newtonian flow behavior of the fiber-reinforced geopolymer mixtures. The model parameters, including yield stress, consistency index, and flow index, aligned well with theoretical expectations;
- The addition of polypropylene fibers significantly influenced the extrusion behavior of the geopolymer composites. Higher fiber contents (PP0.75 and PP1) increased yield stress and viscosity, resulting in extrusion challenges such as material segregation and high extrusion pressures;
- Optimal fiber content ranges (0.25% and 0.5%) were identified, balancing mechanical properties and extrudability. These mixtures demonstrated smooth and continuous extrusion with desirable mechanical properties, making them suitable for 3D printing applications;
- FEM simulations using the COMSOL model showed good alignment with experimental data for low to moderate fiber contents, but deviated at higher fiber contents. This suggests further refinement of the numerical model to capture complex fiber–matrix interactions and thixotropic behavior better.

The findings from this study translate directly to real-world 3D printing applications by clearly understanding how fiber content affects the rheological properties and extrusion be-

havior of geopolymer composites. This knowledge is crucial for optimizing the mix design to ensure the structural integrity and durability of printed components in construction.

**Possible directions for future studies:** Future research could refine FEM models to more accurately simulate fiber–matrix interactions at higher fiber contents. Investigating alternative fibers, such as natural or advanced synthetic fibers and hybrid fiber systems, could enhance geopolymers’ mechanical and rheological properties. Long-term performance studies under various environmental conditions would provide valuable durability data. Scaling up the extrusion process for industrial applications and optimizing fiber content for specific uses are also crucial. Employing advanced characterization techniques, such as micro-computed tomography and scanning electron microscopy, could provide deeper insights into the microstructural changes and fiber distribution within the geopolymer matrix. Addressing high static yield stress and material segregation is essential for future advancements. Additionally, exploring the effects of different mix designs or additive combinations to mitigate high static yield stress could improve extrudability and homogeneity. These efforts will advance the understanding and application of fiber-reinforced geopolymers in construction 3D printing.

**Author Contributions:** Conceptualization, B.S. and A.K.; methodology, B.S.; software, A.K.; validation, B.S. and A.K.; formal analysis, A.K.; investigation, B.S.; resources, B.S.; data curation, B.S., A.K. and M.K.; writing—original draft preparation, B.S. and A.K.; writing—review and editing, B.S. and A.K.; visualization, B.S.; project administration, A.J. and M.K. All authors have read and agreed to the published version of the manuscript.

**Funding:** This research has been funded by the Committee of Science of the Ministry of Science and Higher Education of the Republic of Kazakhstan (Grant No. BR21882278 “Establishment of a construction and technical engineering center to provide a full cycle of accredited services to the construction, road-building sector of the Republic of Kazakhstan”).

**Data Availability Statement:** The data used in this research work can be made available upon request.

**Conflicts of Interest:** The authors declare no conflicts of interest.

## References

1. Jindal, B.B.; Jangra, P. 3D Printed Concrete: A comprehensive review of raw material’s properties, synthesis, performance, and potential field applications. *Constr. Build. Mater.* **2023**, *387*, 131614. [[CrossRef](#)]
2. Zhang, J.; Wang, J.; Dong, S.; Yu, X.; Han, B. A review of the current progress and application of 3D printed concrete. *Compos. Part A Appl. Sci. Manuf.* **2019**, *125*, 105533. [[CrossRef](#)]
3. Kuranlı, Ö.F.; Uysal, M.; Abbas, M.T.; Cosgun, T.; Niş, A.; Aygörmez, Y.; Al-Mashhadani, M.M. Evaluation of slag/fly ash based geopolymer concrete with steel, polypropylene and polyamide fibers. *Constr. Build. Mater.* **2022**, *325*, 126747. [[CrossRef](#)]
4. Dhasindrakrishna, K.; Pasupathy, K.; Ramakrishnan, S.; Sanjayan, J. Rheology and elevated temperature performance of geopolymer foam concrete with varying PVA fibre dosage. *Mater. Lett.* **2022**, *328*, 133122. [[CrossRef](#)]
5. *ASTM C618-19*; Standard Specification for Coal Fly Ash and Raw or Calcined Natural Pozzolan for Use in Concrete. ASTM International: West Conshohocken, PA, USA, 2019.
6. Çevik, A.; Alzebaree, R.; Humur, G.; Niş, A.; Gülşan, M.E. Effect of nano-silica on the chemical durability and mechanical performance of fly ash based geopolymer concrete. *Ceram. Int.* **2018**, *44*, 12253–12264. [[CrossRef](#)]
7. Su, Z.; Hou, W.; Sun, Z. Recent advances in carbon nanotube-geopolymer composite. *Constr. Build. Mater.* **2020**, *252*, 118940. [[CrossRef](#)]
8. Ahmed, H.U.; Mohammed, A.S.; Faraj, R.H.; Qaidi, S.M.; Mohammed, A.A. Compressive strength of geopolymer concrete modified with nano-silica: Experimental and modeling investigations. *Case Stud. Constr. Mater.* **2022**, *16*, e01036. [[CrossRef](#)]
9. Masoud, L.; Hammoud, A.; Mortada, Y.; Masad, E. Rheological, Mechanical, and Microscopic Properties of Polypropylene Fiber Reinforced-Geopolymer Concrete for Additive Manufacturing. *Constr. Build. Mater.* **2024**, *438*, 137069. [[CrossRef](#)]
10. Nematollahi, B.; Vijay, P.; Sanjayan, J.; Nazari, A.; Xia, M.; Nerella, V.N.; Mechtcherine, V. Effect of polypropylene fibre addition on properties of geopolymers made by 3D printing for digital construction. *Materials* **2018**, *11*, 2352. [[CrossRef](#)] [[PubMed](#)]
11. Bellum, R.R. Influence of steel and PP fibers on mechanical and microstructural properties of fly ash-GGBFS based geopolymer composites. *Ceram. Int.* **2022**, *48*, 6808–6818. [[CrossRef](#)]
12. Chhabra, R.P.; Richardson, J.F. *Non-Newtonian Flow and Applied Rheology: Engineering Applications*; Butterworth-Heinemann: Oxford, UK; Waltham, MA, USA, 2011.

13. Nematollahi, B.; Xia, M.; Sanjayan, J.; Vijay, P. Effect of type of fiber on inter-layer bond and flexural strengths of extrusion-based 3D printed geopolymer. In *Proceedings of the Materials Science Forum*; Trans Tech Publications Ltd.: Bäch, Switzerland, 2018; Volume 939, pp. 155–162.
14. Najvani, M.A.D. Early-Age Strength and Failure Characteristics of 3D Printable Polymer Concrete: Numerical Modelling and Experimental Testing. *J. Build. Eng.* **2023**.
15. Khan, S.A.; İlcan, H.; Aminipour, E.; Şahin, O.; Rashid, A.A.; Şahmaran, M.; Koç, M. Buildability analysis on effect of structural design in 3D concrete printing (3DCP): An experimental and numerical study. *Case Stud. Constr. Mater.* **2023**, *19*, e02295. [[CrossRef](#)]
16. Elchalakani, M.; Karrech, A.; Dong, M.; Ali, M.S.M.; Li, G.; Yang, B. Testing and modelling of geopolymer concrete members with fibreglass reinforcement. *Proc. Inst. Civ. Eng.-Struct. Build.* **2021**, *174*, 12–27. [[CrossRef](#)]
17. Murcia, D.H.; Abdellatef, M.; Genedy, M.; Taha, M.M. Rheological Characterization of Three-Dimensional-Printed Polymer Concrete. *ACI Mater. J.* **2021**, *118*, 189.
18. Venkatachalam, S.; Vishnuvardhan, K.; Amarapathi, G.D.; Mahesh, S.R.; Deepasri, M. Experimental and finite element modelling of reinforced geopolymer concrete beam. *Mater. Today Proc.* **2021**, *45*, 6500–6506. [[CrossRef](#)]
19. Pishro, A.A.; Zhang, S.; Hu, Q.; Zhang, Z.; Pishro, M.A.; Zhang, L.; Zhao, Y. Advancing ultimate bond stress–slip model of UHPC structures through a novel hybrid machine learning approach. *Structures* **2024**, *62*, 106162. [[CrossRef](#)]
20. Das, D.; Rout, P.K. Synthesis, characterization and properties of fly ash based geopolymer materials. *J. Mater. Eng. Perform.* **2021**, *30*, 3213–3231. [[CrossRef](#)]
21. Guo, X.; Yang, J.; Xiong, G. Influence of supplementary cementitious materials on rheological properties of 3D printed fly ash based geopolymer. *Cem. Concr. Compos.* **2020**, *114*, 103820. [[CrossRef](#)]
22. Ng, T.S.; Foster, S.J. Development of a mix design methodology for high-performance geopolymer mortars. *Struct. Concr.* **2013**, *14*, 148–156. [[CrossRef](#)]
23. Choi, M.S.; Kim, Y.J.; Kim, J.K. Prediction of concrete pumping using various rheological models. *Int. J. Concr. Struct. Mater.* **2014**, *8*, 269–278. [[CrossRef](#)]
24. Jacobsen, S.; Vikan, H.; Haugan, L. Flow of SCC along surfaces. In *Proceedings of the Design, Production and Placement of Self-Consolidating Concrete: Proceedings of SCC2010, Montreal, QC, Canada, 26–29 September 2010*; Springer: Dordrecht, The Netherlands, 2010; pp. 163–173.
25. Fensterseifer, E.J.; Lima, M.M.; Gleize, P.J.; de Matos, P.R.; Rodríguez, E.D. Fresh properties of fly ash-based geopolymer: The role of the testing conditions on the rheological measurements. *J. Mater. Res. Technol.* **2023**, *26*, 7082–7096. [[CrossRef](#)]
26. Ricciotti, L.; Apicella, A.; Perrotta, V.; Aversa, R. Geopolymer Materials for Extrusion-Based 3D-Printing: A Review. *Polymers* **2023**, *15*, 4688. [[CrossRef](#)] [[PubMed](#)]
27. Liu, J.; Lv, C. Properties of 3D-printed polymer fiber-reinforced mortars: A review. *Polymers* **2022**, *14*, 1315. [[CrossRef](#)] [[PubMed](#)]
28. Zhao, B.; Cheng, Y.; Liu, Y.; Kong, X.; Yang, Z.; Tong, R.; Deng, Y. Investigation of the numerical simulation of debris flow fluid with concern of phase transition. *Front. Earth Sci.* **2022**, *10*, 982332. [[CrossRef](#)]
29. Batchelor, G. *An Introduction to Fluid Dynamics*; Cambridge University Press: Cambridge, UK, 2000.
30. Donea, J.; Huerta, A. *Finite Element Methods for Flow Problems*; Wiley: Hoboken, NJ, USA, 2003.
31. Hughes, T. *The Finite Element Method: Linear Static and Dynamic Finite Element Analysis*; Dover Publications: Mineola, NY, USA, 2000.
32. Nobile, F.; Formaggia, L. A Stability Analysis for the Arbitrary Lagrangian Eulerian Formulation with Finite Elements. *East-West J. Numer. Math.* **1999**, *7*, 105–132.
33. Li, M.; Tang, L.; Xue, F.; Landers, R.G. Numerical Simulation of Ram Extrusion Process for Ceramic Materials. In *Proceedings of the 22nd Annual International Solid Freeform Fabrication Symposium, Austin, TX, USA, 17 August 2011*; University of Texas at Austin: Austin, TX, USA, 2011; pp. 290–308.
34. Hemphill, T.; Campos, W.; Pilehvari, A. Yield-power law model more accurately predicts mud rheology. *Oil Gas J.* **1993**, *91*.
35. Panda, B.; Tan, M.J. Experimental study on mix proportion and fresh properties of fly ash based geopolymer for 3D concrete printing. *Ceram. Int.* **2018**, *44*, 10258–10265. [[CrossRef](#)]

**Disclaimer/Publisher’s Note:** The statements, opinions and data contained in all publications are solely those of the individual author(s) and contributor(s) and not of MDPI and/or the editor(s). MDPI and/or the editor(s) disclaim responsibility for any injury to people or property resulting from any ideas, methods, instructions or products referred to in the content.